Technical Report

Constraining friction properties of mature low-stressed faults such as SAF

SCEC Award #17154, PI Nadia Lapusta

1. Summary of the results

A number of observations suggest (section 3) that well-developed, mature faults such as the San Andreas Fault (SAF) are generally "weak," i.e. operate at low overall levels of shear stress in comparison with what would be expected from Byerlee's law and numerous laboratory experiments on quasi-static or low-slip-rate friction (e.g., Byerlee, 1978; Dieterich, 1979, 1981; Tullis and Weeks, 1986; Blanpied et al., 1991, 1995; Marone, 1998; Wibberley et al., 2008 and references therein). If typical low-slip-rate friction coefficients of 0.6-0.8 are multiplied by overburden minus hydrostatic pore pressure, ~150 MPa at the representative seismic depth of 8 km, one obtains shear strength values of ~100 MPa. Faults that operate at much lower levels of stress (~10-20 MPa) are called "weak" and their strength is called "low."

We have been simulating earthquake sequences in different models for "weak" mature faults aiming to determine which friction and other fault properties in such models are compatible with a range of available general observations such as static stress drops of 1-10 MPa, the observed variations of the breakdown energy and radiated energy with the seismic moment, and the absence of wholesale melting in shear zones. Our eventual goal is to establish which among the acceptable models have behaviors specific to the SAF, including seismic quiescence between large events and paleoseismic data for some SAF segments.

We have found that fault models with rate-and-state friction and additional co-seismic weakening in the form of thermal pressurization of pore fluids are consistent with a number of observations including magnitude-independent stress drops, breakdown energy increasing with the earthquake moment, and radiation ratios of about 0.5 (Figures 1, 2). However, such models, in the parameter regime explored so far, (a) produce mostly crack-like ruptures and (b) result in reasonable stress drops and sub-melting temperature increases for relatively small interseismic effective stresses of 50-100 MPa, which would require chronic fluid overpressure on faults below 3 km or so. We are in the process of examining models with more efficient thermal pressurization and additional stronger co-seismic weakening such as flash heating that have been shown to produce pulse-like ruptures (Figure 3).

To enable comparison of our simulations with observations, we have developed a number of ways of quantifying the observables from our simulations, including stress drop, breakdown energy, and radiation ratio, both (i) directly from the simulated earthquake sources and (ii) indirectly from other observables as it is done for natural earthquakes (Perry et al., 2018; Lin and Lapusta, 2018; Figures 1-4). We are working on developing tools of category (ii) for radiated energy.

2. Relevance of the project goals to the objectives of SCEC

Our project addresses the following SCEC Research Priorities:

P1.c. Constrain how absolute stress and stressing rate vary laterally and with depth on faults

P3.c Assess how shear resistance and energy dissipation depend on the maturity of the fault system

P1.d Quantify stress heterogeneity on faults at different spatial scales

P5.a. Develop earthquake simulators that encode the current understanding of earthquake predictability.

Our study aims to determine which models of low-stresses faults are consistent with basic observations and hence put constraints on the absolute levels of both shear and effective normal stress at all depths, contributing to priority P1.c. Our efforts towards studying the seismological observables and energy

budget for all our simulated events contribute to P3.c. We study how various kinds of heterogeneity on faults translate into nucleation processes and microseismicity, and compare the properties of the resulting microseismicity with observations, constraining the types of heterogeneity, including stress heterogeneity, over the scale of microseismic events, and thus contributing to priority P1.d. We also contribute to P1.d by quantifying the resulting variability of stress before large events. Our goal to produce models of low-stressed SAF segments consistent with basic observations will help towards developing realistic earthquake simulators with predictive power, as in P5.a. The proposed modeling significantly contributes to a number of research priorities of FARM, including "Constrain how absolute stress, fault strength and rheology vary with depth on faults," "Determine how seismic and aseismic deformation processes interact," and "Use numerical models to investigate which fault properties are compatible with paleoseismic findings, including average recurrence, slip rate, coefficient of variation of earthquake recurrence." Confirming that "weak" fault models with low shear stress values are compatible with available observations will contribute to the Community Stress Model.

3. Evidence for "weak" mature faults and two classes of models

The outflow of heat observed for SAF and other mature faults implies that shear stresses acting during sliding are of the order of 10 MPa or less (e.g., Brune et al., 1969; Henyey and Wassenburg, 1971; Lachenbruch and Sass, 1973, Lachenbruch, 1980, Nankali, 2011). Analyses of the fault core obtained by drilling through shallow parts of faults that have experienced major recent events, including the great 2011 Mw 9.0 Tohoku-Oki event, point to co-seismic friction coefficients as low as ~0.1 (e.g., Tanikawa and Shimamoto, 2009; Fulton et al., 2013). Low values for shear stresses acting on major faults including SAF are also supported by the inferences of steep angles between the principal stress direction and fault trace (e.g., Townend and Zoback, 2004; Zoback et al., 2007), significant rotations of principal stress directions due to stress drop in earthquakes as judged by the focal mechanisms of microseismicity (e.g., Wesson and Boyd, 2007), geometry of thrust-belt wedges (e.g., Suppe, 2007), and scarcity of pseudotachylytes, the products of solidifying rock melts (e.g., Sibson, 1975; Rice, 2006).

Two classes of models can explain earthquake occurrence under low shear stress. In the first class, the quasi-static friction is high on average, but fault resistance to slip weakens substantially at seismic slip rates as supported by lab experiments (Tullis, 2015 and references therein; Noda et al., 2009; Noda and Lapusta, 2010, 2013; Jiang and Lapusta, 2016). Earthquake rupture initiates in places of stress concentrations and/or statically weak spots and propagates over the rest of the low-stressed fault due to co-seismic weakening, making the fault appear weak. In the second one, the faults are chronically weak, both during slow (quasi-static) and fast (seismic) slip, due to either low friction coefficients, or low effective normal stress, or both. Such models are supported by low quasi-static friction coefficients for some minerals in the lab (although most of them are also rate-strengthening) and observations of fluid overpressure (e.g., Brown et al., 2003; Faulkner et al., 2006; Bellot, 2008; Bangs et al., 2009; Collettini et al., 2009; Fulton and Saffer, 2009; Carpenter et al., 2011; Lockner et al., 2011). Note that fluid overpressure may be confined to the immediate vicinity of the fault (e.g., Rice, 1992) (and hence not readily observable by bulk velocity studies), due to much higher along-fault permeability compared to the surrounding rock.

While both classes of models can explain fault operation under low shear stress, other aspects of their behavior should exhibit substantial differences. Chronically weak faults operate at the average shear stress levels close to the average static fault strength. For the statically strong but co-seismically weak faults, the average shear stress on the fault is much lower than its average static strength. One expected consequence of this difference is in the temporal and spatial patterns of microseismicity occurrence in the two models (e.g., Jiang and Lapusta, 2016). Another potential difference is in the energy budget and radiation efficiency that we have begun to study in our models.

4. Models with rate-and-state faults and additional co-seismic weakening in the form of thermal pressurization of pore fluids

We have examined long-term earthquake sequences on a rate-and-state fault segment with enhanced dynamic weakening due to thermal pressurization of pore fluids (Perry et al., 2018; Figure 1) using a fully dynamic simulation approach. For computational efficiency, we have considered 2D models with 1D faults. We find that models incorporating enhanced dynamic weakening with thermal pressurization can accommodate common observations, such as magnitude-invariant stress drops, increasing breakdown energy with event size, and radiation efficiencies of approximately 0.5. Previous work (Rice_2006; Viesca and Garagash, 2015) has shown that thermal pressurization of pore fluids can explain the inferred increase in breakdown energy with increasing event size, due to the continuous weakening that occurs with increasing slip (Figure 2). This has been shown using simplified theoretical arguments. As expected based on the prior work, our simulations are able to match the increase in breakdown energy with event size (Figure 1b), first inferred by Abercrombie and Rice (2005) and later further developed by Rice_(2006) and Viesca_and Garagash_(2015).

However, a point of concern has remained as to how to reconcile enhanced dynamic weakening with observations of magnitude-invariant stress drops. As enhanced dynamic weakening results in greater degrees of weakening, with lower final stresses, one would be inclined to expect systematically larger stress drops with increasing event size, under the assumption of comparable levels of prestress. However, our modeling has shown that dynamic weakening can be reconciled with magnitude-invariant stress drops due to larger events having lower average prestress. While small and large events nucleate at locations with similar levels of prestress, what matters is the average prestress at all points involved in the rupture. Smaller events have smaller rupture areas and therefore higher average prestresses that more closely match the prestress of the nucleation zone. Larger events, however, weaken the fault more and propagate further into areas of less favorable (lower) prestress conditions. While the average final stresses for large events including thermal pressurization are indeed lower, our models indicate that the average initial stress is systematically lower as well. We find that the combination of these two effects results in nearly constant average stress drops for events spanning fice orders of magnitude in moment and two orders of magnitude in slip (Figure 1c).

All of our events that rupture only part of the seismogenic domain exhibit magnitude-invariant stress drops; however, ruptures that span the entire velocity-weakening domain do not necessarily follow this trend. We have further investigated how the arrest of such events affects their stress drops. We have found that model-spanning events are influenced by additional factors that do not affect the smaller and medium-sized events, such as being forcibly arrested by the velocity-strengthening regions. The properties of the velocity-strengthening region have an impact on the average stress drop of events that significantly propagate into this region. Varying the velocity-strengthening properties across a range of values is able to produce a range of stress drop behaviors for the largest events. A significantly velocity-strengthening region prevents further rupture propagation and leads to sharply increasing stress drops as events slip more, but are unable to increase their rupture area. A mildly velocity-strengthening region allows for significant propagation and can lead to decreasing stress drops as the event size increases. Moreover, very mildly velocity-strengthening regions that are close to being velocity-neutral may lead to the lowest stress drops for the largest events. Thus, the spatial extent of the ruptured area into velocity-strengthening regions can have an important effect on the overall trend of the observed stress drops.

Another important quantity for describing the dynamic character of an earthquake is the radiation efficiency η, the ratio between the radiated energy E_R and the portion of total strain energy available for radiation and breakdown aka available energy (Venkataraman_and Kanamori,_2004). From an idealized energy budget, the available energy can be seismically estimated using average stress drop and average final slip (Venkataraman_and Kanamori,_2004). Observed radiation efficiencies are often between 0 and 1, and between 0.3 and 0.5 for many large events (Ye_et al._2016a).

We have explored the compatibility of our simulated events incorporating dynamic weakening with these observations of radiation efficiency, as well as the relationship between estimates using this ideal-

ized model with the true radiated energy ratio η_A, which compares the radiated energy with the total available energy throughout the rupture. Our models incorporating enhanced weakening due to only thermal pressurization show similar trends for the seismologically-inferred radiation efficiency, with values approximately around 0.5, consistent with those inferred from large earthquakes by Venkataraman and Kanamori 2004 (Figure 1d). Moreover, for these simulated events, we find consistency between the seismologically-inferred radiation efficiency and the true radiated-energy ratio. This is due to the crack-like nature of these events involving thermal pressurization, with the dynamic levels of stress being nearly equal to the final level of stress, as assumed in the idealized energy considerations (Figure 2). Therefore, we find that models incorporating enhanced dynamic weakening that lead to crack-like styles of rupture are generally consistent with the standard energy budget when considering the averaged rupture behavior.

In summary, our simulations incorporating rate- and state-dependent friction and enhanced dynamic weakening with thermal pressurization are able to match observed trends in increasing breakdown energy with event size, magnitude-invariant stress drops, and seismologically-estimated radiated energy ratios around 0.5. Our stress drops are also consistent with observations of stress drops in the 1-10 MPa range for all of our event sizes, excluding the complete rupture events in some models. Though our models reproduce magnitude-invariant stress drops, the exact mechanism for this remains unknown and is planned for further investigation using our continuing SCEC support. We find that models incorporating enhanced dynamic weakening that lead to crack-like styles of rupture are generally consistent with the standard energy budget when considering the averaged rupture behavior.

5. Models with rate-and-state faults and additional co-seismic weakening in the form of thermal pressurization of pore fluids and flash heating

We have begun to examine the behavior of models that produce much stronger weakening and sharp pulse-like ruptures (Figure 3). Our studies so far have shown that models incorporating enhanced dynamic weakening with thermal pressurization that result in crack-like ruptures tend to be agreeable with the standard considerations for energy partitioning. Such models result in much smaller overshoot or undershoot than their corresponding static stress drop, and therefore remain close to the idealized behavior for which the seismologically estimated quantities are expressed in terms of observable parameters.

More pulse-like ruptures, which can occasionally result from models with thermal pressurization and more reliably in models that incorporate more severe enhanced dynamic weakening such as flash heating, have increasingly more significant undershoot, i.e. the difference between the minimum dynamic and final stress increases (Figure 3). In such cases, the relationship between observable quantities, such as the static stress drop and average slip, with the energy available for breakdown and radiation may not be as apparent. It is commonly suggested that large earthquakes propagate as slip pulses rather than continuously expanding cracks (Heaton 1990; Viesca and Garagash, 2015). It is therefore important to verify that such styles of rupture are consistent with the previously-discussed observed relations that we have already found to be accommodated by crack-like ruptures involving thermal pressurization, namely having magnitude-invariant stress drops, increasing breakdown energy with event size, and radiated energy ratios between 0 and 1. We will continue to explore these rupture modes using our continuing SCEC support.

6. Spectral analysis of microseismicity in our models and sequences on asperity-like fault patches

Using both NSF and SCEC support, we have been developing the methodology for determining seismological observables for small events in our models, in the same way as it is done for natural events (e.g., Madariaga, 1976; Brune, 1970, 1971; Sato and Hirasawa, 1973; Kanamori and Anderson, 1975; Ide and Beroza, 2001; Allmann and Shearer, 2009; Baltay et al., 2011; Hauksson et al., 2012; Lin et al., 2012; Abercrombie, 2014; Kaneko and Shearer, 2014, 2015; Lin et al., 2016). In particular, we have focused on static stress drops, observed to be magnitude-invariant and (nearly) depth-invariant, with typical values of

1-10 MPa for natural earthquakes(Ide and Beroza, 2001; Beroza and Kanamori, 2007, Allmann and Shearer, 2009; Baltay et al., 2011; Hauksson et al., 2012). Since frictional resistance is mostly proportional to the effective normal stress σ, the increase of σ with depth should amplify any stress changes and hence, intuitively, substantially increase static stress drops, but no to mild increases with depth are observed (Shearer et al., 2006; Allmann and Shearer, 2007; Uchide et al., 2014; Goebel et al., 2015; Kita and Katsumata, 2015; Ko and Kuo, 2016; Ye et al., 2016; Abercrombie et al., 2017; Trugman and Shearer, 2017). In our future work, we will simulate microseismicity on "weak" spots of decreased shear strength (e.g., as in Thomas et al., 2014); nucleation-prone spots of modified friction parameters (e.g., as in Jiang and Lapusta, 2016); and normal stress variations motivated by local deviations from fault planarity (e.g., Renard et al., 2006; Sagy et al., 2007; Candela et al., 2009; Brodsky et al., 2011), in models which also have much larger events, to examine the resulting behavior of microseismicity at various depths.

So far, we have considered microseismicity sources in isolation. Observations show that microseismic events from the same fault area can have similar source durations but different seismic moments, violating the commonly assumed scaling (Harrington and Brodsky, 2009; Bouchon et al., 2011; Bostock et al., 2015; Lin et al., 2016). Our numerical simulations of earthquake sequences demonstrate that strength variations over a seismogenic patch provides a potential explanation of such behavior, with the event duration controlled by the patch size and event magnitude determined by how much of the patch area is ruptured (Lin and Lapusta, 2018). We find that the stress drops estimated by typical seismological analyses for the simulated sources significantly increase with the event magnitude, ranging from 0.01 to 10 MPa. At the same time, the actual stress drops determined from the on-fault stress changes are magnitude-independent and ~3 MPa. Our findings suggest that fault heterogeneity results in local deviations in the moment-duration scaling and earthquake sources with complex shapes of the ruptured area, for which stress drops may be significantly underestimated by the current seismological methods.

Publications

Perry, S., N. Lapusta, and V. Lambert, Magnitude-invariant stress drops and increasing breakdown energy in earthquake sequence simulations on rate-and-state faults with thermal pressurization, to be submitted to *J. Geophys. Res.*, 2018.

Lin, Y.-Y. and N. Lapusta, Microseismicity simulated on asperity-like fault patches: on scaling of seismic moment with duration and seismological estimates of stress drops, in revision, *Geophys. Res. Lett.,* 2018.

Presentations

Lin, Y.-Y., and N. Lapusta, Exploring variations of earthquake moment on patches with heteroge-neous strength (Poster presentation), JpGU-AGU joint meeting, Chiba, Japan, May 2017.

Lin, Y.-Y., and N. Lapusta, Comparison of actual and seismologically inferred stress drops in as-perity-type dynamic source models of microseismicity (Poster presentation), SCEC annual meeting, Palm Springs, CA, Sep. 2017.

Schaal, N., N. Lapusta, and Y.-Y. Lin, Exploring seismological properties of asperity-type events in a rate-and-state fault model (Poster presentation), SCEC annual meeting, Palm Springs, CA, Sep. 2017.

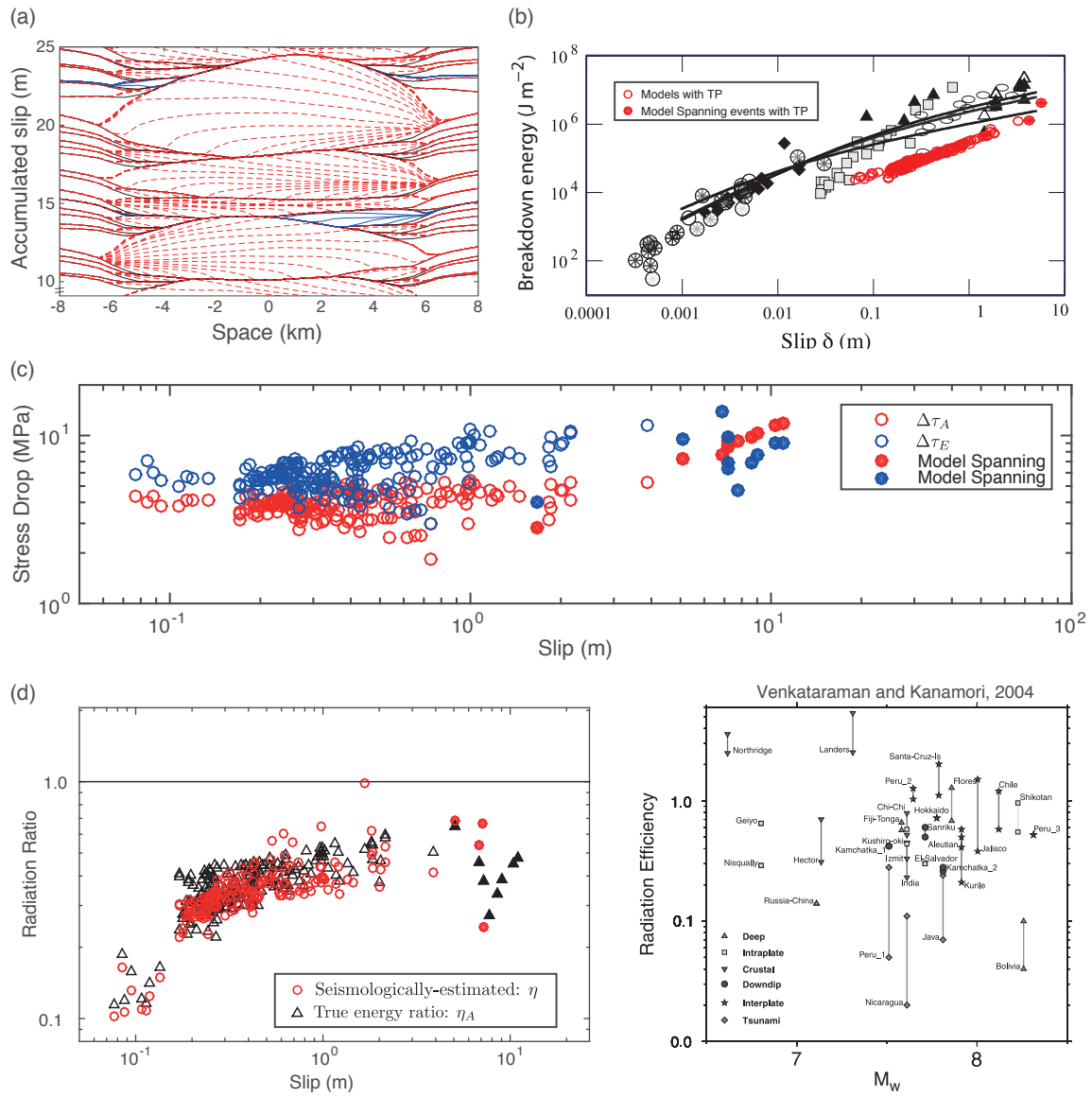

Figure 1. Fault models with rate-and-state friction and additional co-seismic weakening in the form of thermal pressurization of pore fluids are consistent with a number of observations including magnitude-independent stress drops, breakdown energy increasing with the earthquake moment, and radiation ratios of 0.3-1.0 (Perry et al., 2018). (a) Accumulated slip profiles for a portion of the sequence of events produced by a rate-and-state fault model with thermal pressurization in a 12 km velocity-weakening region. (b) Breakdown energies from our simulations compared to those inferred for natural events by Rice (2006). Our models are able to match the trend of the observed events quite well. (c) Stress drops for events in the simulation with thermal pressurization and a 24 km long velocity-weakening region. Complete rupture events have filled-in symbols. d) Seismically estimated radiation ratios (η) and actual radiation ratios η_A vs. average slip (left), in comparison to those inferred from large earthquakes (right) from Venkataraman and Kanamori (2004).

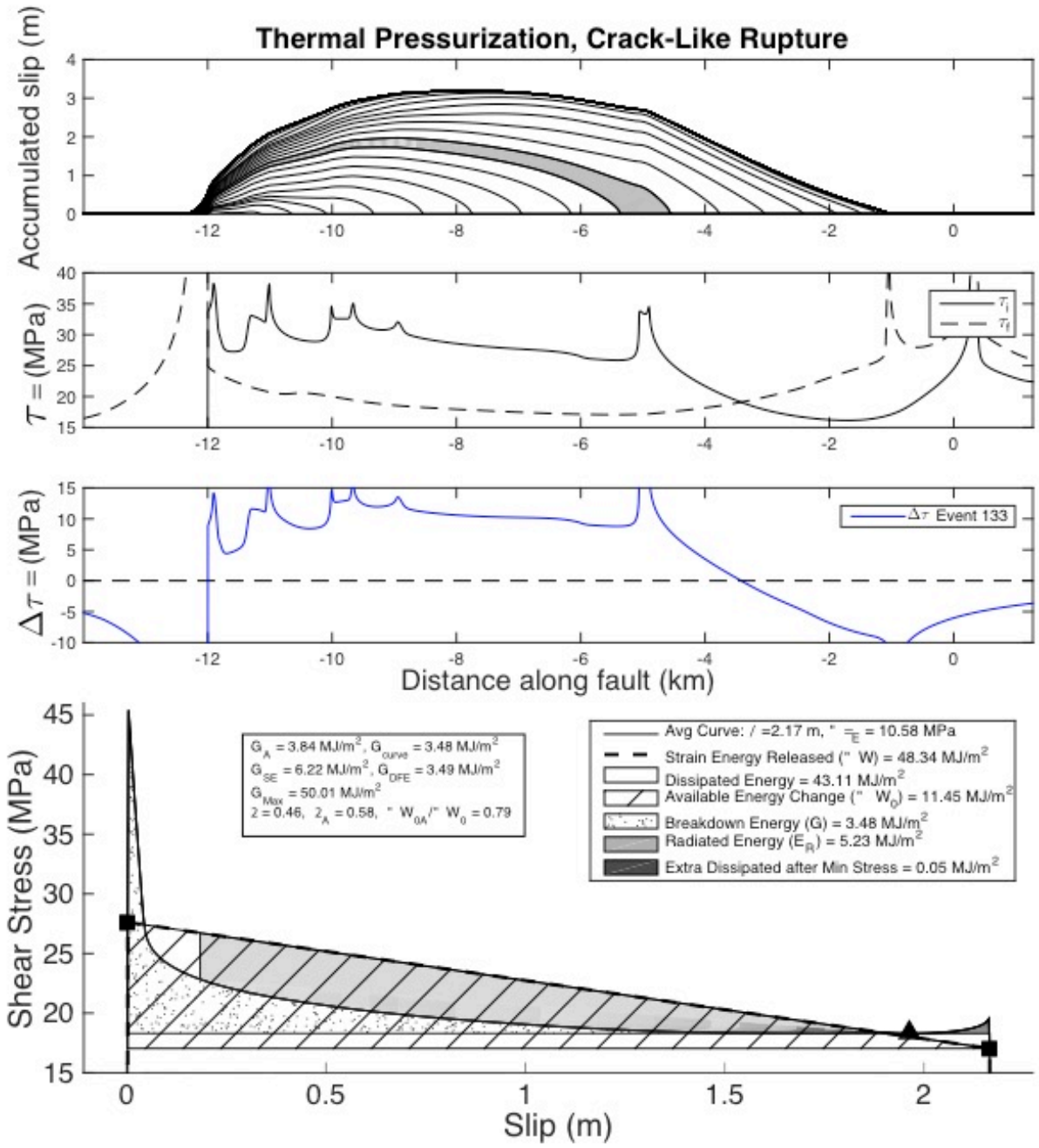

Figure 2. Representative event for crack-like behavior with thermal pressurization. (Row 1) Accumulated slip profile with slip distribution along the fault plotted every 0.5 s. (Row 2) Initial and final stress distributions along the fault. The rupture nucleates in regions of high prestress but subsequently propagate into areas of lower prestress. (Row 3) Stress drop distribution along the fault. Row (4) Average shear stress vs. slip curve with relevant energy quantities labeled. Initial and final stresses are marked with black squares. The actual energy quantities from simulations are close to those obtained from seismological estimates.

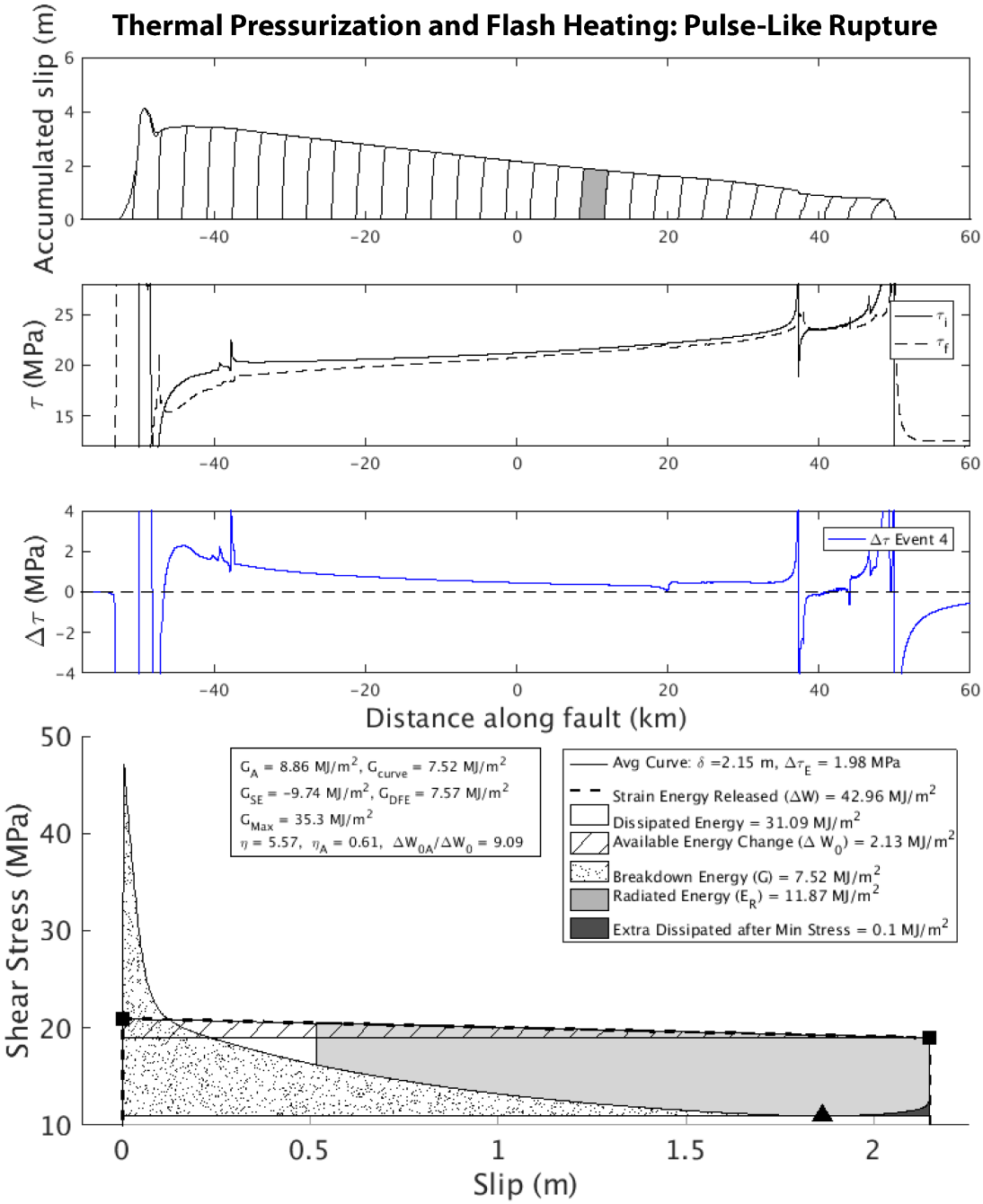

Figure 3. Representative event showing pulse-like behavior. (Row 1) Accumulated slip profile with slip distribution along the fault plotted every 1 s. A portion of slip accumulated is shaded to emphasize the pulse-like behavior. (Row 2) Initial and final stress distributions along the fault. (Row 3) Stress drop distribution along the fault. (Row 4) Average shear stress vs. slip curve with relevant energy quantities labeled. The sharp pulse-like nature of the rupture leads to significant restrengthening and a large stress undershoot at final slip, making the standard energy analysis inaccurate.

References

Abercrombie, R. E., and J. R. Rice (2005), Can Observations of earthquake scaling constrain slip weakening? *Geophys J. Int.*, 162, 406-424, doi: 10.1111/j.1365-246X.2005.02579.x.

Abercrombie, R. E. (2014), Stress drops of repeating earthquakes on the San Andreas Fault at Parkfield, *Geophys. Res. Lett.*, 41, 8784–8791, doi:10.1002/2014GL062079.

Abercrombie, R. E., S. Bannister, J. Ristau, and D. Doser (2017), Variability of earthquake stress drop in a subduction setting, the Hikurangi Margin, New Zealand*, Geophys. J. Int.*, 208, 306-320, doi: 10.1093/gji/ggw393.

Allmann, B. P., and P. M. Shearer (2007), Spatial and temporal stress drop variations in small earthquakes near Parkfield, California, *J. Geophys. Res.,* 112, B04305, doi: 10.1029/2006JB004395.

Allmann, B. P., and P. M. Shearer (2009), Global variations of stress drop for moderate to large earthquakes, *J. Geophys. Res.,* 114**,** B01310, doi:10.1029/2008JB005821.

Baltay, A., S. Ide, G. Prieto, and G. Beroza (2011), Variability in earthquake stress drop and apparent stress. *Geophys. Res. Lett.*, 38, L06303, doi:10.1029/2011GL046698.

Bangs N. L. B., G. F. Moore, S. P. S. Gulick, E. M. Pangborn, H. J. Tobin, S. Kuramoto, and A. Taira, Broad (2009), weak regions of the Nankai Megathrust and implications for shallow coseismic slip, *Earth. Planet. Sci. Lett.*, 284, 44-49.

Bellot, J. P. (2008), Hydrothermal fluids assisted crustal-scale strike-slip on the Argentat fault zone, *Tectonophysics*, 450, 21-33.

Beroza, G. C., and H. Kanamori (2007), Earthquake Seismology: Comprehensive Overview, *Treatise on Geophysics*, Volume 4: Earthquake Seismology, 9. 1-58, edited by G. Schubert, Elsevier.

Blanpied, M. L., D. A. Lockner, and J. D. Byerlee (1991), Fault stability inferred from granite sliding experiments at hydrothermal conditions, *Geophys. Res. Lett.*, 18(4), 609-612.

Blanpied, M. L., D. A. Lockner, and J. D. Byerlee (1995), Frictional slip of granite at hydrothermal conditions, *J. Geophys. Res*., 100, 13045-13064.

Brodsky, E. E., J. J. Gilchrist, A. Sagy, and C. Collettini (2011), Faults smooth gradually as a function of slip, *Earth. Planet. Sci. Lett.*, 302(1-2), 185–193, doi:10.1016/j.epsl.2010.12.010.

Bostock, M. G., A. M. Thomas, G. Savard, L. Chuang, and A. M. Rubin (2015), Magnitudes and moment-duration scaling of low-frequency earthquakes beneath southern Vancouver Island, *J. Geophys. Res.*, 120(9), 6329-6350.

Bouchon, M., H. Karabulut, M. Aktar, S. Özalaybey, J. Schmittbuhl, and M. P. Bouin (2011), Ex-tended nucleation of the 1999 Mw 7.6 Izmit earthquake, *Science*, 331(6019), 877-880, doi:10.1126/science.1197341.

Brown, K. M., A. Kopf, M. B. Underwood, and J. L. Weinberger (2003), Compositional and fluid pressure controls on the state of stress on the Nankai subduction thrust: A weak plate boundary, *Earth. Planet. Sci. Lett.*, 214, 589-603.

Brune, J. N., T. L. Henyey, and R. F. Roy (1969), Heat Flow, Stress, and Rate of Slip along the San Andreas Fault, California, *J. Geophys. Res.*, 74(15), 3821–3827.

Brune, J. (1970), Tectonic stress and the spectra of seismic shear waves from earthquakes, *J. Geophys. Res.*, 75, 4997–5009, doi:10.1029/JB075i026p04997.

Brune, J. N. (1971), Correction, *J. Geophys. Res.*, 76, 5002.

Byerlee, J. D. (1978), Friction of rocks, *Pure and Applied Geophysics,* 116, 615–626, doi:10.1007/BF00876528.

Candela, T., F. Renard, M. Bouchon, A. Brouste, D. Marsan, J. Schmittbuhl, and C. Voisin (2009), Characterization of Fault Roughness at Various Scales: Implications of Three-Dimensional High Resolution Topography Measurements, *Pure Appl. Geophys.*, 166(10), 1817–1851.

Carpenter, B. M., C. Marone, and D. M. Saffer (2011), Weakness of the San Andreas Fault revealed by samples from the active fault zone, *Nature Geosci.,* 4, 251–254.

Collettini, C., A. Niemeijer, C. Viti, and C. Marone (2009), Fault zone fabric and fault weakness, *Nature,* 462, 907-910.

Dieterich, J.H. (1979), Modeling of rock friction, 1. Experimental results and constitutive equations, *J. Geophys. Res*., 84, 2161–2168.

Dieterich, J.H. (1981), Constitutive properties of faults with simulated gouge, in Mech. BehaviorCrustal Rocks, edited by N.L. Carter et al., *Geophys. Monogr. Ser.,* 24, 103–120. AGU, Washington,D.C.

Faulkner D. R., T. M. Mitchell, D. Healy, and M. J. Heap (2006), Slip on 'weak' faults by the rotation of regional stress in the fracture damage zone, *Nature,* 444, 922-925.

Fulton, P. M. and D. M. Saffer (2009), Potential role of mantle-derived fluids in weakening the San Andreas Fault, *J. Geophys. Res.*, 114, B07408.

Fulton, P.M., E. E. Brodsky, Y. Kano, J. Mori, F. Chester, T. Ishikawa, R. N. Harris, W. Lin, N. Eguchi, and S. Toczko (2013), Expedition 343, 343T, and KR13-08 Scientists, Low Coseismic Friction on the Tohoku-Oki Fault Determined from Temperature Measurements, *Science*, 342, 1214-1217.

Goebel, T. H. W., E. Hauksson, P. M. Shearer, and J. P. Ampuero (2015), Stress-drop heterogeneity within tectonically complex regions: a case study of San Gorgonio Pass, southern California, *Geophys. J. Int.*, 202, 514-528, doi: 10.1093/gji/ggv160.

Hauksson, E., W. Yang, and P. M. Shearer (2012), Waveform Relocated Earthquake Catalog for Southern California (1981 to June 2011), *Bull. Seismol. Soc. Am.*, 102(5), 2239–2244, doi:10.1785/0120120010.

Heaton, T.H. (1990), Evidence for and implications of self-healing pulses of slip in earthquake rupture. Phys. Earth Planet. Inter., 64, 1-20.

Henyey, T. L. and G. J. Wasserburg (1971), Heat Flow near Major Strike-Slip Faults in California, *J. Geophys. Res.*, 76(32), 7924–7946.

Harrington, R. M., and E. E. Brodsky (2009), Source duration scales with magnitude differently for earthquakes on the San Andreas Fault and on secondary faults in Parkfield, California. *Bull. Seismol. Soc. Am.*, 99(4), 2323-2334, doi:10.1785/0120080216

Ide, S., and G. C. Beroza (2001), Does apparent stress vary with earthquake size? *Geophys. Res. Lett.*, 28(17), 3349-3352.

Jiang, J., and N. Lapusta (2016), Deeper penetration of large earthquakes on seismically quiescent faults, *Science*, 352, 1293-1297, doi:10.1126/science.aaf1496.

Kanamori, H., and D. L. Anderson (1975), Theoretical basis of some empirical relations in seismology, *Bull. Seismol. Soc. Am.*, *65*,1073–1095.

Kaneko, Y., and P. M. Shearer (2014), Seismic source spectra and estimated stress drop derived from cohesive-zone models of circular subshear rupture, *Geophys. J. Int.*, 197, 1002–1015, doi:10.1093/gji/ggu030.

Kaneko, Y., and P.M. Shearer (2015), Variability of seismic source spectra, estimated stress drop, and radiated energy, derived from cohesive-zone models of symmetrical and asymmetrical circular and elliptical ruptures, *J. Geophys. Res.,* 120, 1053-1079, doi:10.1002/2014JB011642.

Kita, S., and K. Katsumata (2015), Stress drops for intermediate-depth intraslab earthquakes beneath Hokkaido, northern Japan: Differences between the subducting oceanic crust and mantle events, *Geochem. Geophys. Geosyst.*, 16, 552-562, doi:10.1002/2014GC005603.

Ko, J. Y.-T., and B.-Y. Kuo (2016), Low radiation efficiency of the intermediate-depth earthquakes in the Japan subduction zone, *Geophys. Res. Lett*., 43, 11611-11619, doi: 10.1002/2006GL070993.

Lachenbruch, A.H., and J. H. Sass (1973), Thermo-mechanical aspects of the San Andreas fault system, *in* Kovach, R L., and Nur, Amos, eds., Proceedings of the conference on tectonic problems of the

San Andreas fault system: Stanford, Calif., Stanford University Publications in the Geological Sciences, 13, 190-205.

Lachenbruch, A. H. (1980), Frictional heating, fluid pressure and the resistance to fault motion, *J. Geophys. Res*., 85, 6097-6112.

Lin, Y.-Y., K.-F. Ma, and V. Oye (2012), Observation and Scaling of Microearthquakes from Taiwan Chelungpu-fault Borehole Seismometers, *Geophys J. Int.,*190, 665–676, doi: 10.1111/j.1365-246X.2012.05513.x.

Lin, Y.-Y., K.-F. Ma, H. Kanamori, T.-R. A. Song, N. Lapusta, and V. C. Tsai (2016), Evidence for Non-Self-similarity of Microearthquakes Recorded at the Taiwan Borehole Seismometer Array, *Geophys J. Int.,* 206, 757-773.

Lin, Y.-Y., and N. Lapusta (2018), Microseismicity simulated on asperity-like fault patches: on scaling of seismic moment with duration and seismological estimates of stress drops, in revision, *Geophys. Res. Lett.*

Lockner, D. A., C. Morrow, D. Moore, and S. Hickman (2011), Low strength of deep San Andreas fault gouge from SAFOD core, *Nature*, 472, 82-85.

Madariaga, R. (1976), Dynamics of an expanding circular crack, *Bull. Seismol. Soc. Am.*, 66, 639–666.

Marone, C. (1998), Laboratory-derived friction laws and their application to seismic faulting, *Ann. Revs. Earth & Plan. Sci.*, 26, 643-696.

Nankali, H. R. (2011), Slip rate of the Kazerun Fault and Main Recent Fault (Zagros, Iran) from 3D mechanical modeling, *J. Asian Earth Sci.*, 41, 89-98.

Noda, H., E. M. Dunham, and J. R. Rice (2009), Earthquake ruptures with thermal weakening and the operation of major faults at low overall stress levels, *J. Geophys. Res.*, 114, B07302, doi:10.1029/2008JB006143.

Noda, H., and N. Lapusta (2010), Three-dimensional earthquake sequence simulations with evolving temperature and pore pressure due to shear heating: Effect of heterogeneous hydraulic diffusivity, *J. Geophys. Res*., 115(B12), B12314, doi:10.1029/2010JB007780.

Noda, H. and N. Lapusta (2012), On averaging interface response during dynamic rupture and energy partitioning diagrams for earthquakes, *J. Appl. Mech.*, 79, 031026, doi:10.1115/1.4005964.

Noda, H., and N. Lapusta (2013), Stable creeping fault segments can become destructive as a result of dynamic weakening, *Nature*, 493, pp. 518-521.

Noda, H., N. Lapusta, and H. Kanamori (2013), Comparison of average stress drop measures for ruptures with heterogeneous stress change and implications for earthquake physics, *Geophys. J. Int.*, 193, 3, 1691-1712, doi:10.1093/gji/ggt074.

Perry, S., N. Lapusta, and V. Lambert (2018), Magnitude-invariant stress drops and increases in breakdown energy in earthquake sequence simulations on rate-and-state faults with thermal pressurization, to be submitted to *J. Geophys. Res.*

Renard, F., C. Voisin, D. Marsan, and J. Schmittbuhl (2006), High resolution 3D laser scanner measurements of a strike-slip fault quantify its morphological anisotropy at all scales, *Geophys. Res. Lett*., 33(4), L04305.

Rice, J. R. (1992), Fault Stress States, Pore Pressure Distributions, and the Weakness of the San Andreas Fault, in *Fault Mechanics and Transport Properties in Rocks*, edited by B. Evans and T.-F. Wong, Academic Press, 475-503.

Rice J. R. (2006), Heating and weakening of faults during earthquake slip, *J. Geophys. Res*., 111, B05311, doi:10.1029/2005JB004006.

Sagy, A., E. E. Brodsky, and G. J. Axen (2007), Evolution of fault-surface roughness with slip, *Geology*, 35, 283-286.

Sato, T., and T. Hirasawa (1973), Body wave spectra from propagating shear cracks, *J. Phys. Earth*, *21*, 415–431.

Shearer, P. M., G. A. Prieto, and E. Hauksson (2006), Comprehensive analysis of earthquake source spectra in southern California, *J. Geophys. Res.*, 111, B06303, doi: 10.1029/2005JB003979.

Sibson, R. H. (1975), Generation of pseudotachylyte by ancient seismic faulting, *Geophys. J. R. Astron. Soc.,* 43, 775– 794.

Suppe, J. (2007), Absolute fault and upper crustal strength from wedge tapers, *Geology,* 35, 1127-1130.

Tanikawa, W., and T. Shimamoto (2009), Frictional and transport properties of the Chelungpu fault from shallow borehole data and their correlation with seismic behavior during the 1999 Chi-Chi earthquake. *J. Geophys. Res.*, 114(B1), doi:10.1029/2008JB005750.

Thomas M. Y., N. Lapusta, H. Noda, and J.-P. Avouac (2014), Quasi-dynamic versus fully-dynamic simulations of earthquakes and aseismic slip with and without enhanced coseismic weakening, *J. Geophys. Res*.,119, 1986-2004.

Townend J., and M. D. Zoback (2004), Regional tectonic stress near the San Andreas fault in central and southern California, *Geophys. Res. Lett*., 31 (15), L15S11.

Trugman, T., and P. M. Shearer (2017), Application of an improved spectral decomposition method to examine earthquake source scaling in Southern California, *J. Geophys. Res*., 122, 2890-2910, doi: 10.1002/2017JB13971.

Tullis, T. E. and J. D. Weeks (1986), Constitutive behavior and stability of fictional sliding in granite, *Pure Appl. Geophys.*, 124, 383-414.

Tullis, T. E. (2015), Mechanisms for friction of rock at earthquake slip rates, in *Treatise on Geophysics (second edition),* vol. 4, Earthquake Seismology, edited by H. Kanamori, Elsevier, Oxford, 139-159.

Uchide, T., P. M. Shearer, and K. Imanishi (2014), Stress drop variations among small earthquakes before the 2011 Tohoku-oki, Japan, earthquake and implications for the main shock, *J. Geophys. Res*., 119, 7164-7174, doi:10.1002/2014JB010943.

Venkataraman, A., & Kanamori, H. (2004). Observational constraints on the fracture energy of subduction zone earthquakes, *J. Geophys. Res*., *109*(B5), doi: 10.1029/2003JB002549.

Viesca, R. C., & Garagash, D. I. (2015), Ubiquitous weakening of faults due to thermal pressurization. *Nature Geoscience*, *8*(11), 875-879, doi:10.1038/ngeo2554.

Wesson, R. L., and O. S. Boyd (2007), Stress before and after the 2002 Denali fault earthquake, *Geophys. Res. Lett.,* 34, L07303.

Wibberley, C. A. J., G. Yielding, and G. Di Toro (2008), Recent advances in the understanding of fault zone structure, in The Internal Structure of Fault Zones: Implications for Mechanical and Fluid‐Flow Properties, pp. 5–33, Geol. Soc. of London, London.

Ye, L., T. Lay, H. Kanamori, and L. Rivera (2016), Rupture Characteristics of Major and Great (Mw ≥ 7) Megathrust Earthquakes from 1990-2015: 2. Depth Dependence, *J. Geophys. Res*., 121, 845-863.

Zoback, M. D., S. Hickman, and W. Ellsworth (2007), The role of fault zone drilling, in *Treatise on Geophysics*, vol. 4, Earthquake Seismology, edited by H. Kanamori, Elsevier, Amsterdam.